Development and testing of a microwave-heated plasma thruster

IEPC-2024-217

Presented at the 38th International Electric Propulsion Conference, Toulouse, France
June 23-28, 2024

Jens Schmidt* and Clara E. Schäfer† and Yung-An Chan‡ and Felix Plettenberg§
and Martin Grabe¶
German Aerospace Center (DLR), Institute of Aerodynamics and Flow Technology,
Department of Spacecraft, Bunsenstr. 10, 37073 Göttingen, Germany

Within the Decentralized Energy Electric Propulsion (DEEP) project a microwave-heated plasma thruster is developed. The thruster is operated intermittently in combination with a battery and supercapacitor. This allows the use of a battery and solar panel system designed for a lower power on the satellite itself as well as a reduction in overall mass, therefore increasing the available payload mass and power. Due to the intermittent operation, the thruster needs to ignite fast and reliable, while each firing will only last $\tau = 10 - 600$ s depending on the duty cycle and necessary velocity increment Δv. The thruster itself consists of an electron-cyclotron-resonance (ECR) discharge in combination with a magnetic nozzle for plasma acceleration. The accelerated plasma is therefore quasi-neutral and no neutralizer is necessary. Erosion of the components exposed to the plasma is minimized. In addition to the thruster, a flow management system (FMS) and power control and distribution unit (PCDU) are developed from commercial off-the-shelf components.

Nomenclature

B = Magnetic field strength
E = Electric field
E_e = Effective electric field
e = Elementary charge
F = Thrust
f = Frequency
I_sp = Specific Impulse
$\dot{m}$ = Mass flow rate
m_e = Electron mass
P = Power
$\dot{V}$ = Volume flow rate
S_{11} = Scattering parameter
η = Total Efficiency
ω = Angular frequency
ω_c = Electron cyclotron frequency
ν_e = Electron collision frequency

*Research Associate, jens.schmidt@dlr.de
†Doctoral Student, clara.schaefer@dlr.de
‡Research Associate, yung-an.chan@dlr.de
§Student, felix.plettenberg@dlr.de
¶Group Leader 'Rarefied Flows', martin.grabe@dlr.de

Copyright 2024 by the Electric Rocket Propulsion Society. All rights reserved.

I. Introduction

Current in-orbit electric propulsion has several drawbacks: The necessity for rare and expensive noble gases such as xenon and krypton as a propellant, the necessity for neutralizers which limit the possible propellants, and the decrease of performance over lifetime due to erosion. Within the *Decentralized Energy Electric Propulsion* (DEEP) project[7] a microwave-heated plasma thruster with the name DEEVA (DLR Electrodeless ECR Via Microwave Plasma Accelerator) is developed. For the DEEP mission, the thruster is operated intermittently in combination with a battery and supercapacitor. This allows the use of a battery and solar panel system designed for a lower power on the satellite itself as well as a reduction in overall mass, therefore increasing the available payload mass and power. Due to the intermittent operation, the thruster needs to ignite fast and reliable, while each firing will only last $\tau = 10 - 600$ s, depending on the duty cycle and necessary velocity increment Δv. In addition, the steady-state condition of the thruster has to be reached in a short time-frame. The thruster is aimed to produce a thrust of $F = 1$ mN at a specific impulse of $I_s = 1000$ s with xenon at a power of $P = 100$ W. The thruster itself consists of an electron-cyclotron-resonance (ECR) discharge heated by microwaves in combination with an divergent magnetic field acting as magnetic nozzle for plasma acceleration. The magnetic nozzle converts the thermal energy of the electrons into directed kinetic energy of the ions. The accelerated plasma is therefore quasi-neutral and no neutralizer is necessary. All surfaces which are exposed to the plasma consist of quarz-glass and in addition, the magnetic field necessary for the discharge and acceleration also confines the plasma and minimizes wall losses. Erosion of the components exposed to the plasma is minimized. Due to this configuration, the thruster lifetime can be extended, as also the erosion and deposition of metals should be reduced, slowing the decrease in the performance over time. Additionally, the electrodeless discharge and acceleration allow a high flexibility in propellants, although the performance for different propellants might vary. In addition to the thruster, a flow management system (FMS) and power control and distribution unit (PCDU) are developed from commercial off-the-shelf components. Within this work, the development and initial testing and measurements of the thruster shall be described.

II. Fundamentals

The DEEVA thruster, as shown schematically in Fig. 1, consists of several components: the circular waveguide antenna with a microwave launcher and two slits propagating the wave into the discharge tube, the quartz-glass discharge tube separating the plasma from the antenna, a gas injector, two neodymium magnets which provide a strong enough magnetic field for ECR to occur and a ferrite ring magnet is used to create the convergent-divergent magnetic field for plasma acceleration. It also guides the magnetic field lines within the discharge tube and achieve additional confinement of the plasma. The magnets can be oriented with the same or alternating polarity. The antenna itself is manufactured out of aluminum to decrease cost and weight, while for the microwave feeder a commercially available N-type socket is used on which a copper antenna is screwed or soldered. In the current version, the antenna is stabilized by four threaded rods which compress the front- and back of the antenna. These will be removed in the final qualification model but allow easy modification of the thruster and its components as magnets can be easily added or removed. To reduce the thermal strain on the magnets, the neodymium magnets providing the strong field for the ECR condition are placed outside of the discharge tube. Since the magnetic field decreases cubically with the distance to the source $\vec{r}^3$, the gas injector is designed to be very thin and allow penetration of the magnetic field into the discharge tube. The neutral gas is injected along the outer radius along multiple equidistant boreholes to produce a homogeneous neutral gas distribution within the discharge tube.

To obtain the ECR discharge in the microwave regime, the microwaves are at the same frequency as the cyclotron frequency of the electrons as given by Eq. 1, in which e is the elementary charge, B is the absolute value of the magnetic field and m_e is the electron mass. Additionally, the wave propagation vector needs to be right-handedly polarized and orthogonal to the direction of the magnetic field. The ECR condition can either be achieved by creating the right magnetic field B or coupling at the right frequency $\omega_c = 2\pi f$.

$$\omega_\mathrm{c} = \frac{eB}{m_\mathrm{e}} \tag{1}$$

For a frequency of $f = 2.45$ GHz as given from the frequency limit of the used microwave generator, Eq. 1 results in a necessary magnetic field strength of $B = 87.5$ mT, which is reached roughly at the center of the antenna. The average absorbed power P_{abs} per volume at a coordinate $\vec{r}$ is found from Korzec[2,4] to be

Copyright 2024 by the Electric Rocket Propulsion Society. All rights reserved.

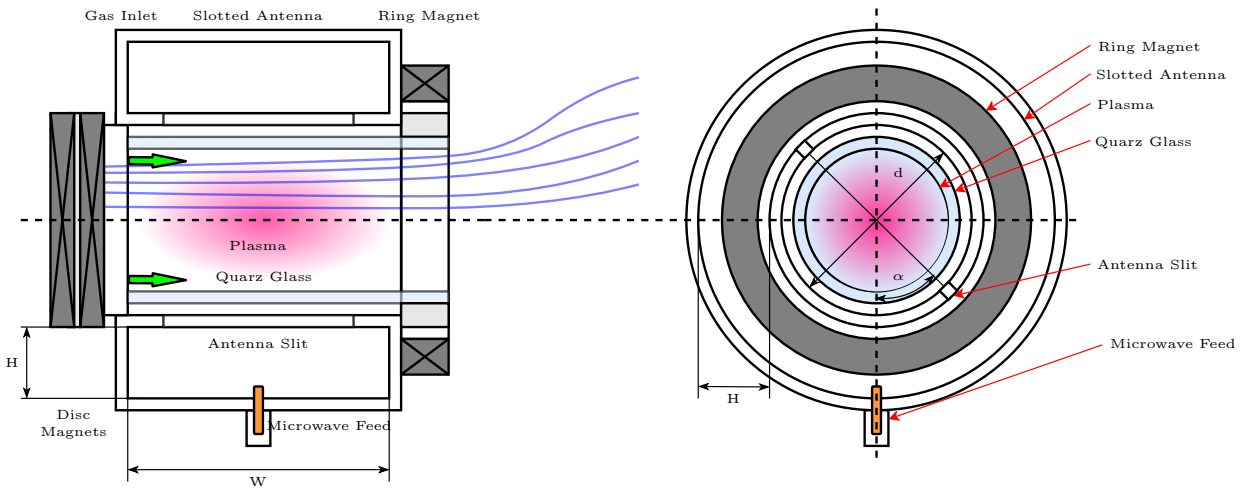

Figure 1. Scheme of the DEEVAv2 thruster with slotted antenna and magnet configuration as seen from the side (left) and front (right) with magnetic field lines (blue). Not to scale. Shown parameters are diameter of the cavity d, height of the slotted waveguide H, length of the slotted waveguide L, and the angle between the feeder and the first slot α.

a function of electron density n_e, electron collision frequency ν_e and effective electric field E_e as given in Eq. 2:

$$P_{\mathrm{abs}}(\vec{r}) = \frac{n_{\mathrm{e}}(\vec{r})e^2}{2m_e\nu_{\mathrm{e}}}|E_{\mathrm{e}}(\vec{r})|^2. \tag{2}$$

The effective electric field $|E_{\mathrm{e}}(\vec{r})|$ can be found from

$$|E_{\mathrm{e}}(\vec{r})|^2 = \frac{\nu_{\mathrm{e}}^2}{2}\Big(\frac{1}{\nu_{\mathrm{e}}^2+(\omega-\omega_{\mathrm{c}})^2}+\frac{1}{\nu_{\mathrm{e}}^2+(\omega+\omega_{\mathrm{c}})^2}\Big)|E(\vec{r})|^2 \approx \frac{\nu_{\mathrm{e}}^2}{\omega^2}|E(\vec{r})|^2 \tag{3}$$

in which ω_{c} is the electron cyclotron frequency. As it can be seen from Eq. 2, the absorbed power increases with increasing electron density n_e and decreasing collision frequency ν_e. The collision frequency decreases also with decreasing pressure, therefore the absorbed power is increased for lower pressures. Furthermore Eq. 2 shows that the absorbed power is strongly dependent on the effective electric field $|E_e(\vec{r})|^2$, therefore it is necessary to maximize the electric field to couple power efficiently into the discharge. Since the absorbed power also depends on the electron density, which strongly increases once a plasma is ignited, the plasma can be sustained at much lower powers after a successful ignition. The magnetic field is designed in such way, that at the exit area of the thruster, a magnetic field strength of $B = 10$ mT is achieved.[3,5]

III. Simulation of the electromagnetic field propagation

To determine the geometrical parameters of the slotted antenna (SLAN),[10] the propagation of the electromagnetic high-frequency field was simulated using COMSOL Multiphysics 6.0[1] within the frequency range of $f = 2.4 - 2.5$ GHz. For this parameter study, four free parameters were used: Diameter of the cavity d, Height of the slotted waveguide H, Length of the slotted waveguide L, and the angle between the feeder and the first slot α. A scheme of the front view of the antenna is shown in Fig. 5. As a measure of performance, the S_{11}-parameter is used. It is defined in Eq. 4 as the ratio and incident wave a_1 and outgoing wave b_1 at port 1, the microwave feed of the slotted antenna.

$$S_{11} = \frac{a_1}{b_1}\Big|_{a_2=0} = \frac{V_1^-}{V_1^+} \tag{4}$$

Furthermore, the influence of slot length l and width w as well as feed diameter and length were studied. During the numerical analysis of the antenna, several possible geometries and a strong dependence of the S_{11}-parameter on the angle α in the range of $25 < \alpha < 60$ ° were found. A typical mode for the electric

Copyright 2024 by the Electric Rocket Propulsion Society. All rights reserved.

and magnetic field is shown in Fig. 2. As it can be seen, the dominant mode within the inner cavity is a TE_{21} mode,[6] which also seems to be the mode of the outer annular waveguide. In addition, the magnitude of the electric field E is plotted for an input power of $P_{\mathrm{MW}} = 50$ W. As it can be seen, the electric field strength is the highest close to the two opposing slits of the annular waveguide. This also means, that the discharge tube should be large enough in diameter so that the highest density of the neutral gas is in the same location as the maximum of the field strength, resulting in much better coupling of the microwave into the plasma. The finalized antenna was manufactured in a design which allowed easy modification of the geometrical antenna parameters, since the angle α between the microwave launcher and slots as well as the distance of the back-wall s of the cavity could be modified. This allowed tuning of the antenna using a vector-network analyzer to optimize power coupling and compensate for manufacturing tolerances. For the manufactured model, the S_{11} parameter as defined in eq. 4 was measured using a *Rigol DSA800* virtual network analyzer. The result of the measurement and the simulation result of the same geometry are displayed in Fig. 3. The measurement result is shown in blue curve with the standard deviation over multiple dis- and reassembles of the antenna, while the simulation result is shown in orange. As it can be seen, the shape of the function is very similar, resembling the shape of a microwave resonator[6] while being significantly smaller for the desired wavelength in comparison to a normal circular resonator. The minimum is shifted by around $\Delta f \approx 15$ MHz, this is most likely due to the non-ideality of the real antenna in terms of surface properties and manufacturing tolerances of the geometry. In addition, the simulated geometry was simplified in comparison to the real antenna to reduce computational costs and allow easier parametrization and reduce the degrees of freedom. Furthermore, the material constants might differ between simulation and experiment. Considering these effects, the agreement is surprisingly good, as both minima are in the range of the possible frequencies of the used microwave generator, therefore the simulated antenna geometry is actually usable in practice.

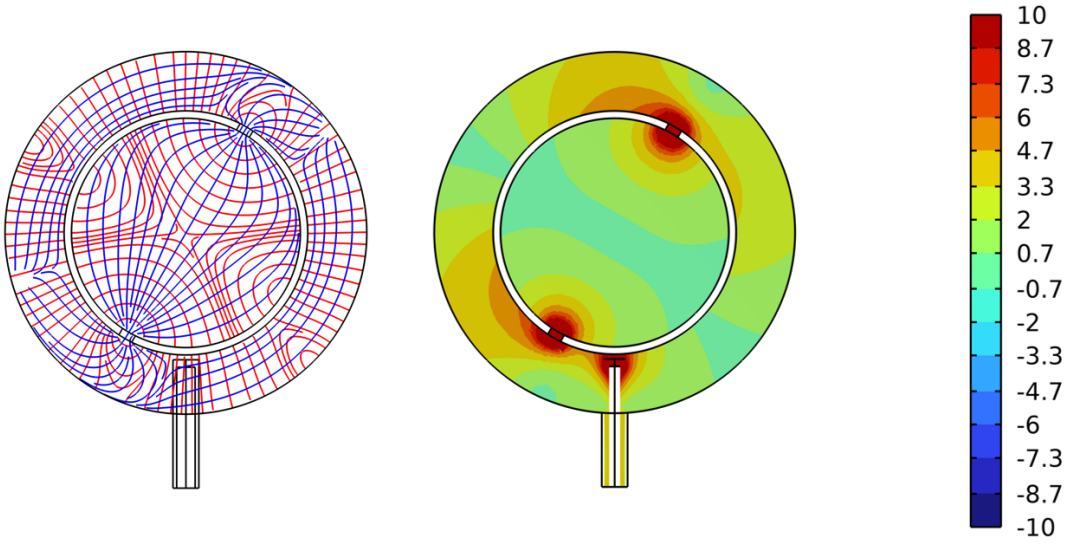

Figure 2. Streamlines of the electric (red) and magnetic (blue) field at $z = W/4$ (left) and absolute value of the electric field (right) in 10^4 V m^{-1} for an input power of $P_{\mathrm{MW}} = 50$ W for the configuration of $\alpha = 30°$ from simulations in COMSOL. Simulation without quartz-glass tube.

IV. Experimental results

The thruster was operated within the STG-MT ('Simulation facilty for thrusters Göttingen - miniature thrusters') vacuum chamber on top of a thrust balance[8] as shown in Fig. 4. To produce the microwave signal, a *KU SG 2.45-250 A* microwave generator was used, which is capable to operate at powers of up to $P_{\mathrm{fwd}} = 250$ W which in practice was limited to $P_{\mathrm{fwd}} = 120$ W due to constraints of the used DC power supply. The power to the thruster was transmitted through a RG400 cable and a vacuum feedthrough. Alternatively, the power can be transferred buy using two circular waveguides acting as sender and receiver as shown in

Copyright 2024 by the Electric Rocket Propulsion Society. All rights reserved.

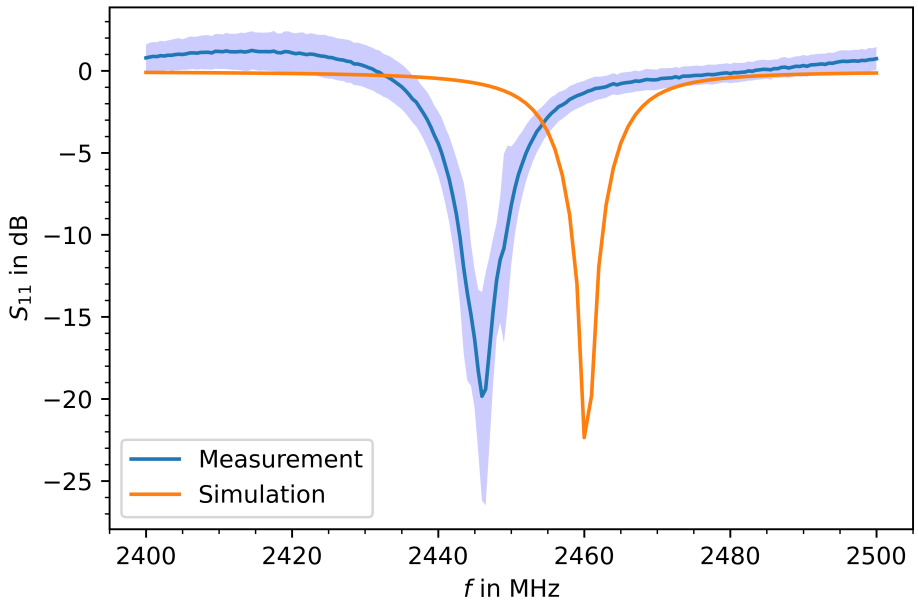

Figure 3. S_{11} **parameter in dB of the antenna as a function of the frequency** f **in** MHz **from simulation results (orange) and measurements (blue, with standard deviation).**

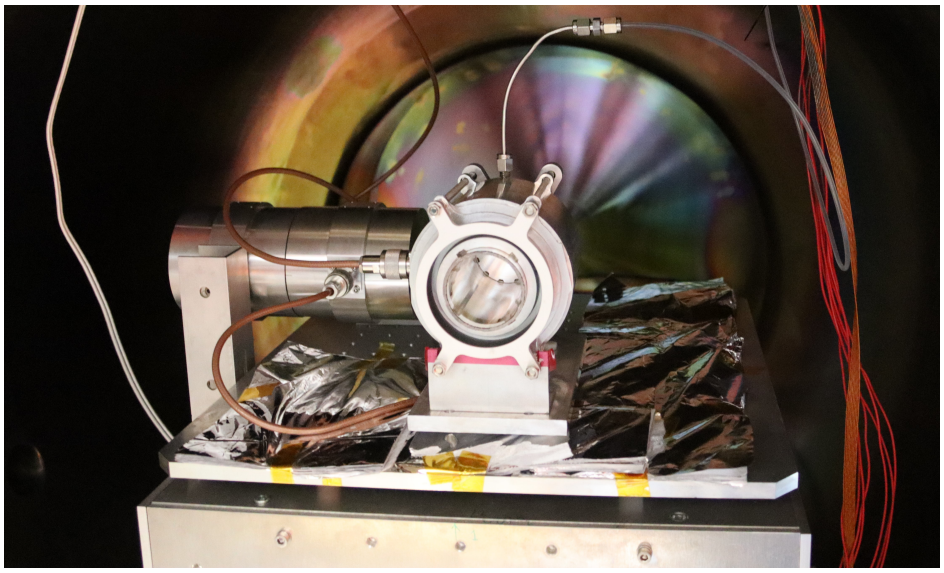

Figure 4. Thruster within the STG-MT facility on top of the thrust balance with circular waveguides for power transmission (left) and gas feed line (top).

Copyright 2024 by the Electric Rocket Propulsion Society. All rights reserved.

the picture opposing on the thrust balance and the chamber to minimize errors in the thrust measurement due the thermal expansion of the cable. It has to be noted, that for both cases there is a significant loss of microwave power within the transmission line, which is even higher for the circular waveguides.

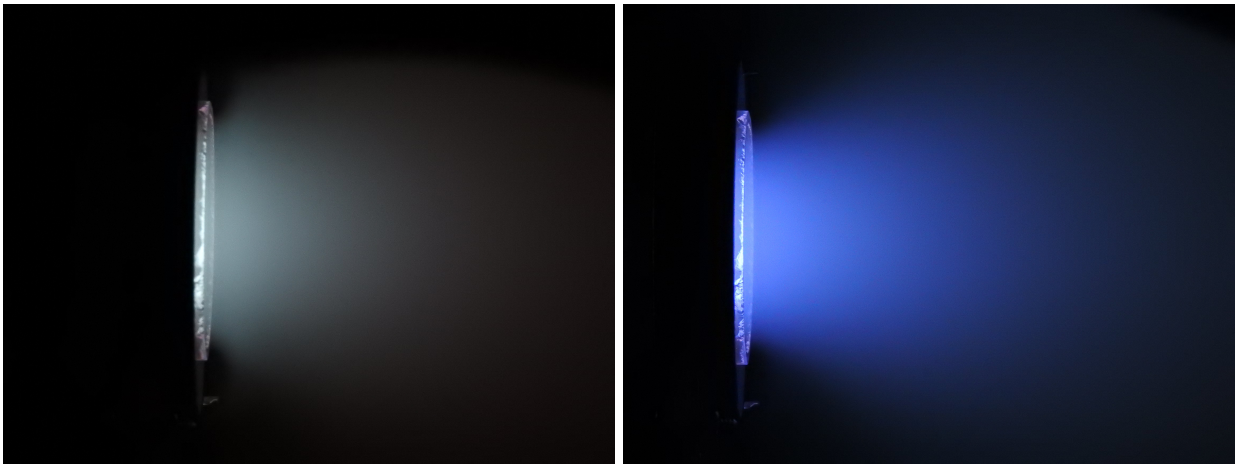

Figure 5. Thruster in operation with xenon at $P = 30$ W and $\dot{V} = 1$ sccm (left) and argon at $P = 60$ W and $\dot{V} = 2$ sccm (right).

The thruster in operation with xenon can be seen on the left in Fig. 5. The divergence of the plume is clearly visible, but also close to the exit plane of the discharge tube the effect of the magnetic field on confining the plasma at a distance from the discharge tube is obvious. It was operated continuously for up to $\tau = 3600$ s, after which the thruster was shut off to not exceed the maximum operation temperature of the neodymium magnets. It was operated at microwave power levels between $P_{\mathrm{MW}} = 20 - 120$ W with volume flows of $\dot{V} = 1 - 45$ sccm of argon and xenon. As seen on the right in Fig. 5, the thruster was also operated with argon as a more cost-effective alternative for testing and operation, leading to a slightly different shape of the plume. Furthermore, the operation with krypton and air was demonstrated. For ignition a power of $P_{\mathrm{MW}} = 60$ W is necessary, which can be decreased to $P_{\mathrm{MW}} = 20$ W once the plasma is ignited. The reflected power P_{ref} depended on the thruster temperature T_T, volume flow rate $\dot{V}$ and frequency f. After ignition, the frequency f at which ideal coupling ($P_{\mathrm{ref}} \leq 1$ W) is shifted due to the microwave absorption and reflection of the plasma, but still within the range of the microwave generator. Therefore, during operation the frequency is changed until the reflected power is minimized. One of the reasons for the change of the reflected power and ideal coupling frequency over time is most probably the change of the antenna geometry as the thruster temperature changes, leading to a change thruster length and cavity diameter. By increasing the thruster efficiency and lowering the losses into the thruster structure, the change in temperature should be decreased and a more stable operation should be possible. Thrust measurements were performed using argon. To explore the parameter space, the power P, frequency f and volume flow $\dot{V}$ were varied. In the present data, thrust measurements were carried out by directly connecting the thruster to the vacuum feedthrough using a microwave cable. Some results of the thrust measurements are shown in Fig. 6 in which the thrust F is plotted against the coupled in microwave power P_{MW} for argon at a volume flowrate of $\dot{V} = 1$ sccm in two configurations using the same ferrite magnet. In the first configuration, both magnets were aligned in the same direction, in the other, the magnets were aligned to be repulsive. As it can be seen, for both configurations, the thrust increases with the power. For the attracting configuration of the magnets, the thrust was higher and increases stronger than for the repulsive configuration. A maximum thrust of $F = 0.36$ mN was measured for a power of $P_{\mathrm{MW}} = 70$ W. There were no thrust measurements performed for microwave powers above $P_{\mathrm{MW}} > 70$ W. A decrease in thrust with increase of the volume flow above $\dot{V} > 2$ sccm was observed. This is most likely due to the loss of electron energy by collisions with neutrals as the number density inside of the discharge tube increases. For the variation of the frequency, it was found that the thrust changes with the frequency with the same dependence as the S_{11} parameter changes with f as shown in Fig. 3. Therefore, the thrust increases with better coupling of the microwaves into the antenna and hence better coupling into the discharge. The plasma parameters of the plume were studied using a Langmuir probe and retarding potential analyzer resulting in an ion energy of around $E_{i,max} = 100$ eV for argon,[9] while the ion energies for xenon were significantly lower.

Copyright 2024 by the Electric Rocket Propulsion Society. All rights reserved.

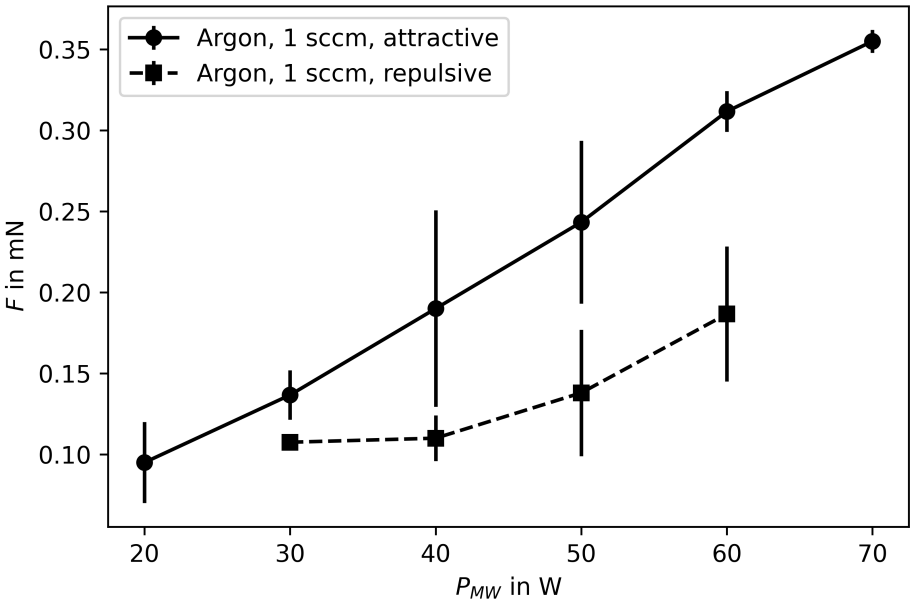

Figure 6. Measured thrust F as a function of microwave power P_{MW} for argon at a volume flow rate of $\dot{V} = 1$ sccm in the configuration with attracting (circles, solid) and repulsive (squares, dashed) magnets. Error bars depict standard deviation.

V. Conclusion

A microwave-heated plasma source applicable for electric space propulsion was designed, the wave propagation inside of the antenna was simulated and the source was tested successfully with the antenna and magnets in vacuum with different propellants. From numerical simulations and experimental testing an ideal angle α between launcher and slots as well as a ideal dimension for the other free parameters of the antenna was found. Direct thrust measurements were performed using a thrust balance, resulting in a maximum thrust of $F = 0.36$ mN for a microwave input power of $P_{\mathrm{MW}} = 70$ W.

$$\eta = \frac{F^2}{2P_{\mathrm{MW}}\dot{m}} \tag{5}$$

Using the expression 5, a maximum efficiency of $\eta = 0.03$ can be found for this power in the current configuration, while for a power of $P_{\mathrm{MW}} = 30$ W only an efficiency of $\eta = 0.01$ was found. Since the efficiency seems to increase with microwave power, it might be promising to perform future tests at higher powers and confirm this result. The measured thrust of P_{MW} corresponds to a specific impulse of $I_{sp} \approx 1200$ s. Two magnetic field configurations were studied, of which one produces less thrust due to the non-optimal field topology. Stable and repeatable ignition and operation for the necessary period of $\tau = 10 - 600$ s was demonstrated, while a strong dependency of the reflected power on the frequency f could be observed. The thruster efficiency needs to be increased to become comparable to other microwave thrusters. This will be done by modifying the topology of the magnetic field to increase the ECR region and achieve a better performance of the magnetic nozzle. In addition, the performance with xenon and other alternative propellants should be studied further. Future optimization is possible by decreasing the antenna geometry, allowing the use onboard small satellites or CubeSats to increase mission lifetimes.

Copyright 2024 by the Electric Rocket Propulsion Society. All rights reserved.

Acknowledgments

The authors would like to thank Kalle Bräumer for performing the thrust measurements with argon.

References

[1]COMSOL Multiphysics® v. 6.2. www.comsol.com. COMSOL AB, Stockholm, sweden.

[2]J. Engemann, M. Schott, F. Werner, and D. Korzec. Large volume electron cyclotron resonance plasma generation by use of the slotted antenna microwave source. *Journal of Vacuum Science & Technology A*, 13(3):875–882, May 1995.

[3]J. Y. Kim, K.-J. Chung, K. Takahashi, M. Merino, and E. Ahedo. Kinetic electron cooling in magnetic nozzles: experiments and modeling. *Plasma Sources Science and Technology*, 32(7):073001, July 2023. Publisher: IOP Publishing.

[4]D. Korzec, F. Werner, A. Brockhaus, J. Engemann, T. P. Schneider, and R. J. Nemanich. Characterization of a slot antenna microwave plasma source for hydrogen plasma cleaning. *Journal of Vacuum Science & Technology A*, 13(4):2074–2085, July 1995.

[5]J. M. Little and E. Y. Choueiri. Thrust and efficiency model for electron-driven magnetic nozzles. *Physics of Plasmas*, 20(10):103501, Oct. 2013. Number: 10 Publisher: American Institute of Physics.

[6]D. M. Pozar. *Microwave Engineering*. John Wiley & Sons, Nov. 2011. Google-Books-ID: _YEbGAXCcAMC.

[7]J. Schmidt, J. Simon, and M. Grabe. The DEEP Thruster Concept. In IEPC, editor, *37th International Electric Propulsion Conference 2022*, pages 1–9, Boston, June 2022.

[8]J. Schmidt, J. Simon, and A. Neumann. Thrust measurements of the RIT-10 thruster with a new type of thrust balance. *International Journal of Energetic Materials and Chemical Propulsion*, 22(4), 2023. Publisher: Begel House Inc.

[9]C. E. Schäfer, J. Schmidt, F. Plettenberg, Y.-A. Chan, M. Grabe, and J. Martinez-Schramm. Comparative Study of Electron Temperature and Ion Energy in Two Different Magnetic Nozzle Thruster Designs. In *Proceedings of the 38th International Electric Propulsion Conference*, volume 154, Toulouse, France, June 2024. Electric Rocket Propulsion Society.

[10]F. Werner, D. Korzec, and J. Engemann. Surface wave operation mode of the slot antenna microwave plasma source SLAN. *Journal of Vacuum Science & Technology A*, 14(6):3065–3070, Nov. 1996.

Copyright 2024 by the Electric Rocket Propulsion Society. All rights reserved.